OBSERVATION OF NONLINEAR COUPLING OF WAVES EXCITED AT DISTINCT REGIONS OF OVERLAPPING DUAL LOWER HYBRID AND ION CYCLOTRON RESONANCES

H. IGAMI,
National Institute for Fusion Science,
Toki-city, Japan
Email: igami.hiroe@nifs.ac.jp

M. TOIDA
National Institute for Fusion Science,
Toki-city, Japan

A. FUKUYAMA
Graduate School of Engineering Kyoto University,
Kyoto-city, Japan

S. INAGAKI
Institute of Advanced Energy, Kyoto University,
Uji-city, Japan

R. SEKI, H. YAMAGUCHI
National Institute for Fusion Science
The Graduate University for Advanced Studies, SOKENDAI
Toki-city, Japan

Y. KATOH
Graduate School of Science, Tohoku University
Sendai-city, Japan

Abstract

This study shows the evidence of the non-linear coupling between waves in the lower hybrid (LH) and its harmonic frequency range excited spontaneously at spatially separated regions in a magnetically confined fusion-oriented (MCF) plasma with existence of energetic ions. (i) Burst-like emissions of waves in LH frequency (f_0) and their harmonic frequency ranges accompanied by sidebands with two distinct ion cyclotron (IC) frequency range intervals f_1, and f_2 were observed. (ii) Bicoherence analysis revealed that LH and its harmonic range waves (lf_0) nonlinearly coupled with the sidebands ($mf_0 \pm nf_1$, $mf_0 \pm nf_2$) characterized by f_1 and f_2. (iii) Two spatially separated "dual resonances", namely DR1 and DR2 were identified in the main confinement region. The LH resonance (LHR) of f_0 overlaps with the ion cyclotron resonance (ICR) of f_1 at DR1 and the LHR of f_0 overlaps with the ICR of f_2 at DR2. This fact that waves, which can potentially contribute to the resonant heating of bulk ions, spontaneously grow nonlinearly due to the presence of high-energy ions and distinct spatially separated dual resonances, has a significant impact on exploring scenarios for sustaining fusion burning plasmas

1. INTRODUCTION

Understanding of the energy cascade process of energetic ions is an important issue for fusion plasma research. If we can find a scenario where fusion born alpha particles excite waves that resonantly heat bulk ions, efficient sustainment of the burning plasma can be expected. Interaction of alpha particles with lower hybrid (LH) waves and ion Bernstein waves in fusion plasmas have been studied theoretically [1-4]. Nonlinear first-principles simulations demonstrated that stimulated fast Alfvén wave emission whose frequency is $18\omega_{c\alpha}$ caused by population inversion in the velocity space of fusion-born alpha particles enhance the externally applied weak fast Alfvén wave of $18\omega_{c\alpha}$ and increase the energy density of the thermal majority deuterons [5].

In magnetically confined fusion (MCF) plasmas, an analogous energetic ion population can be realized by neutral beam injection (NBI). Observation of waves and their interactions originated from beam ions are instructive for studying the energy cascade process of alpha particles via waves. In the Large Helical Device (LHD), emissions of ion cyclotron (IC) and its harmonic range, namely ion cyclotron emissions (ICEs) have been observed in variety types of plasma discharges with NBI [6-12]. Not only ICEs but also waves in LH frequency range have been

observed [8, 12] in LHD. Waves in the LH frequency range detected during perpendicular NBI were interpreted as magnetosonic mode [13]. While waves in LH frequency range observed during the start-up phase of the plasma discharges initiated with tangential NBI and electron cyclotron resonance heating (ECRH), that consist of characteristic spectrograms: spectral peaks shifted in a stair-like manner with increasing density, were interpreted that ion cyclotron waves (ICWs) and ion Bernstein waves (IBWs) were excited in the core region of the plasma. Electromagnetic particle-in-cell (PIC) simulations using with assuming local plasma parameters near the magnetic axis and a ring-like velocity distribution of energetic ions demonstrated that ion Bernstein waves (IBWs), with dispersion coupled to LH waves, can be excited by energetic ions, yielding spectra with peaks close to integer multiples of the IC frequency [14]. PIC simulations have also demonstrated that LH harmonic range waves can be excited by energetic ions with sidebands whose gaps correspond to the IC frequency [15].

In LHD, LH harmonic range waves have been observed with sidebands whose intervals are almost correspond with IC frequency when the stair-like spectrogram mentioned above appears. We have also found that the emission intensity shows burst-like modulations. Numbers of sidebands appear during large bursts. Previous PIC simulations using local plasma parameters did not capture the burst-like behavior in the simulation period less than 100 ion cyclotron period. The period of the burst seen in the experiments are approximately 10^4 times of ion cyclotron period, namely several kHz. In this paper, characteristics of nonlinear coupling between waves are investigated. During large bursts, a wave in LH frequency range interacts with distinct ion cyclotron frequencies.

2. RESULTS

2.1. Observation of stair-like spectrogram during the plasma start-up phase

Antennas to detect high frequency electric fluctuations up to 2 GHz are installed in a vacuum vessel port viewing a viewing the horizontal cross section (10-O port) and a port viewing a longitudinal cross section (9.5-L port) in LHD. During the plasma start-up phase with simultaneous tangential hydrogen NBI with 164 keV/3.86 MW and ECRH with 154 GHz/2.0 MW in total from $t = 3.30$ *s*, semi periodic burst-like emissions were detected in the LH frequency (~200 MHz) and their harmonic frequency ranges accompanied with sidebands with frequency intervals of IC frequency range (30~40 MHz) in Fig.1-(b) and Fig.2-(b). In this experiment, the magnetic configuration was (R_{ax}, B_t) = (*3.90 m, 2.538 T*) where R_{ax} is the distance from the center of the torus to the magnetic axis and B_t is the magnetic field strength at the magnetic axis. As the background plasma density increases, higher hydrogen IC harmonic frequency appears in order like stairs. As mentioned previously, the previous PIC simulation study shows that the IC harmonic wave with $\omega \simeq l\omega_{ci}$, is excited when the lower hybrid wave with ω_{LH} approaches $l\,\omega_{ci}$ in the presence of energetic ions.

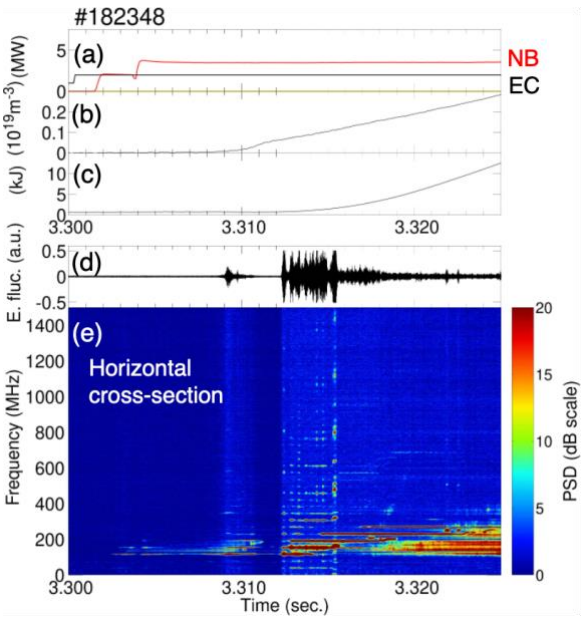

Figure 1: Time change of (a) heating power, (b) line averaged density, (c) stored energy, (d) electric fluctuation signal and (e) frequency spectrogram detected in a port viewing a horizontally long cross section (10-O port)

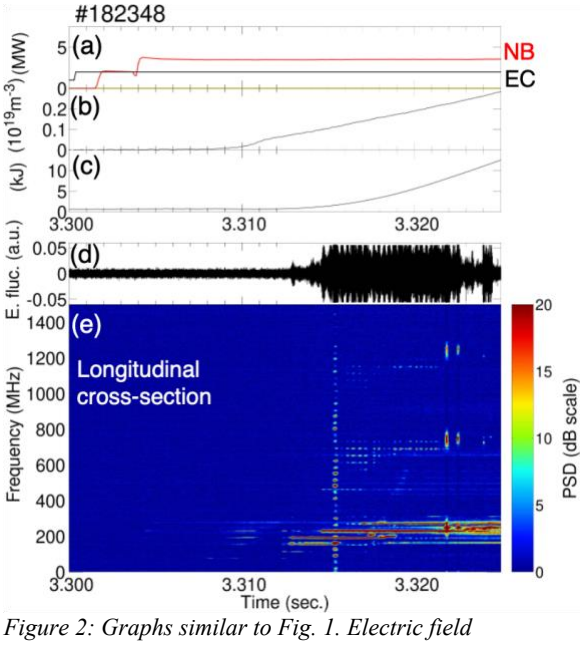

Figure 2: Graphs similar to Fig. 1. Electric field fluctuation is detected in a port viewing a longitudinal cross section (9.5-L port).

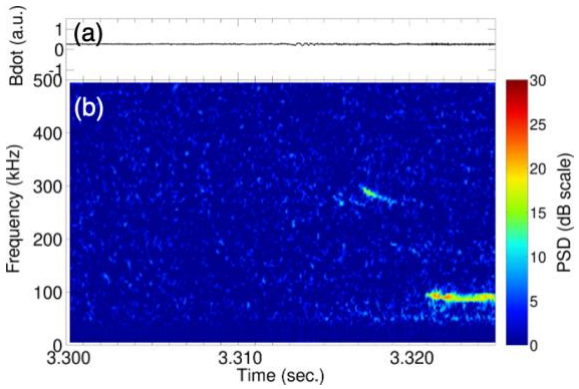

Figure 3: Time change of (a) magnetic fluctuation detected by Mirnov coil, and (b) the spectrogram

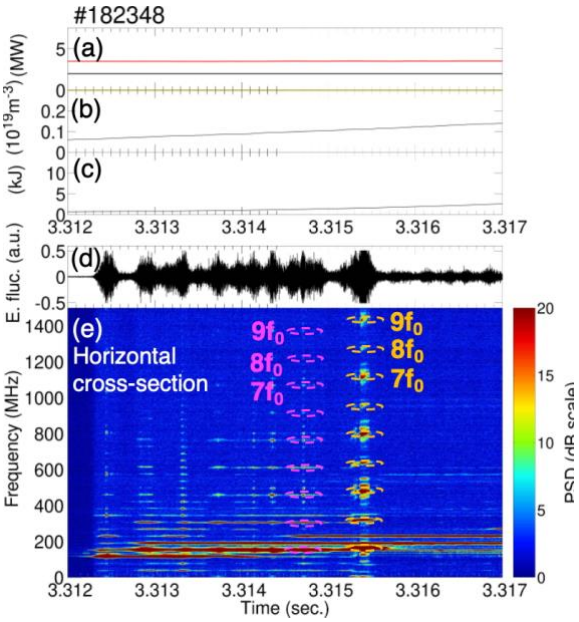

Figure 4: Time expanded view of Fig.1. Before the largest burst, harmonics of f_0=152.5 MHz are shown in the frequency spectrogram (e) with sidebands during bursts. During the largest burst, harmonics of f_0=159.167 MHz with sidebands.

Fig. 3 shows magnetic fluctuations detected by a Mirnov coil input to a digitizer of 1 MHz sampling and its frequency spectrogram. Different from previous observations of ICEs with large intensity burst synchronized with bursty MHD events, such as toroidal Alfvén eigenmode (TAE) [7, 12], tongue-shaped magnetic surface deformation with subsequent energetic-ion-driven MHD mode (EIC) [11], no apparent magnetic fluctuations synchronized with excited MHz range waves were detected during the stair-like spectrogram with semi-periodic burst-like intensity enhancements are observed.

2.2. Interactions between excited waves

When the whole emission intensity is bursty increased, intense peaks of the frequency spectrum appear at multiples of a lower hybrid frequency range wave f_0. Large number of sidebands appear around f_0 and nf_0. Fig. 4 shows the time expanded views of Fig. 1. The

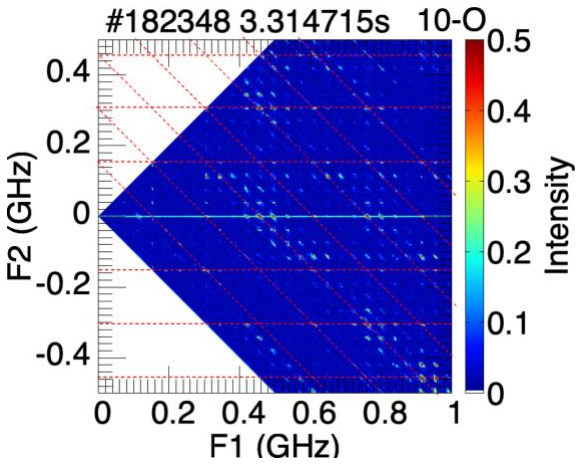

Figure 5: Auto bicoherence of electric fluctuation during a burst around t=3.314715s detected at the 10-O port viewing a horizontally long cross section. Red lines are drawn with gaps of 152.5 MHz

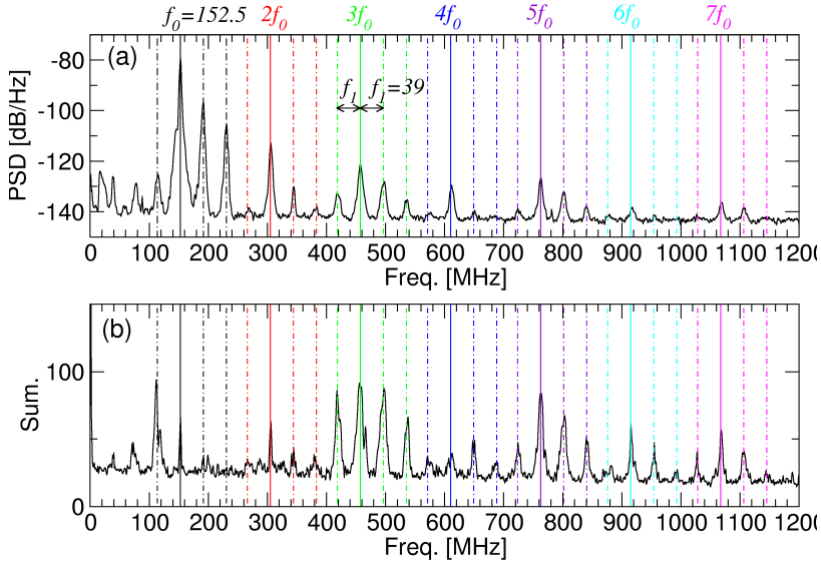

Figure 6: (a) Frequency spectrum averaged around t=3.314715, detected at the 10-O port viewing a horizontal long cross section. (b) Sum of the auto bicoherence. Intense peaks appear around f_0=152.5 MHz and their harmonics with sidebands whose gap frequency f_1 is 39 MHz. In the graphs, dot-dashed lines are drawn with gaps of f_1.

whole emission intensities detected at the 10-O port viewing a horizontally long cross section during bursts was larger before the largest burst around $t=3.31540\ s$ than those after the largest burst. Harmonics of $f_0=152.5\ MHz$ are shown with sidebands during bursts that appear before the largest bursts. Fig. 5 shows the auto bicoherence of the electric field fluctuations detected during a burst around $t=3.314715\ s$. It is shown that harmonics of $f_0=152.5\ MHz$ and their sidebands interact with each other. Fig. 6 shows the intensity and summed auto bicoherence plotted along the frequency. It is clearly shown that the sidebands appear around nf_0 with a constant gap frequency of *39 MHz*.

While the whole emission intensities during bursts detected at the 9.5-L port viewing a longitudinal cross section, became larger after the emission intensity at 230 MHz increases from $t=3.3145\ s$. as shown in Figs. 7. Different from the observation near a horizontal long cross section, odd harmonics of $f_0=230\ MHz$, only appear with sidebands. Fig. 8 shows the auto bicoherence of the electric field fluctuations during a burst around $t=3.31613\ s$ after the largest burst. Interactions between sidebands around odd harmonics and even harmonics are strong. As a result, the spectrum of the sum of bicoherence shows peaks around odd harmonics as shown in Fig. 9-(b). Note that the sums of bicoherence at sidebands around $f_0=230\ MHz$, are larger than that just at $f_0=230\ MHz$. Also, in the observation at the 10-O port viewing a horizontal long cross section, interactions between the even and odd harmonics of $f_0=152.5\ MHz$, are dominant and emission intensities around odd harmonics are larger than those around the even harmonics.

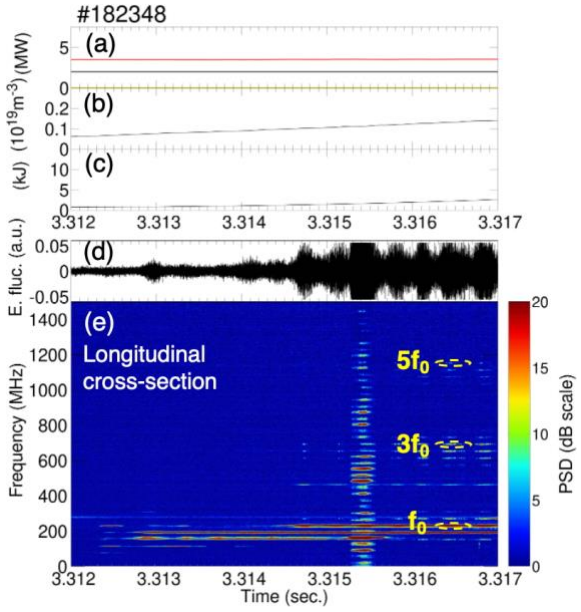

Figure 7: Time expanded view of Fig.2. After t=3.3145s, harmonics of $f_0=230$ MHz are shown with sidebands during bursts.

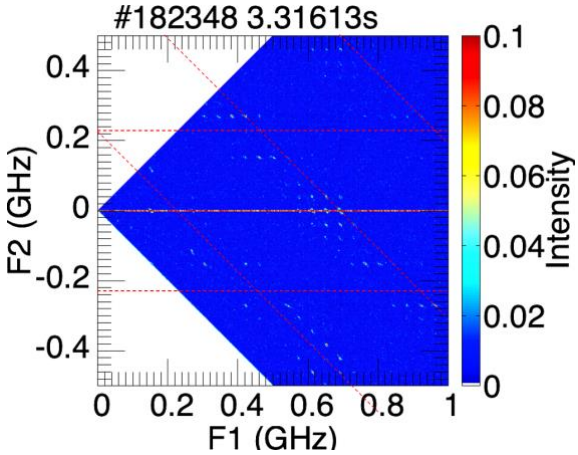

Figure 8: Auto bicoherence of electric fluctuation during a burst around t=3.31613s detected at the 10-O port viewing a horizontally long cross section. Red lines are drawn with gaps of 230 MHz

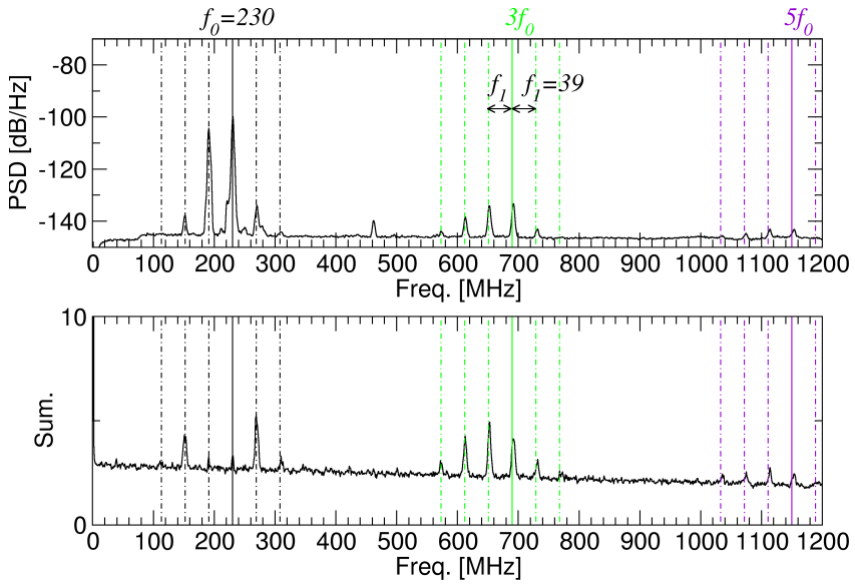

Figure 9: (a) Frequency spectrum averaged around t=3.31613, detected at the 9.5-L port viewing a longitudinal cross section. (b) Sum of the auto bicoherence. Intense peaks appear around $f_0=230$ MHz and their harmonics with sidebands whose gap frequency f_1 is 39 MHz. In the graphs, dot-dashed lines are drawn with gaps of f_1.

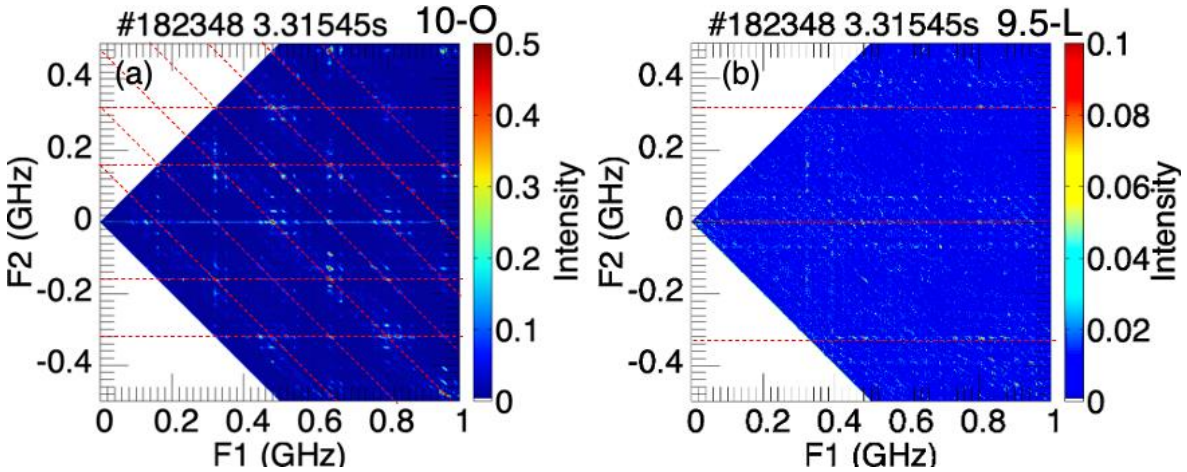

Figure 10: Auto bicoherence of electric fluctuation during the largest burst around t=3.31545s; (a) detected at the 10-O port viewing a horizontally long cross section, with red lines drawn with gaps of 160 MHz; (b) detected at the 9.5-L port viewing a longitudinal cross section with red lines drawn with 320 MHz.

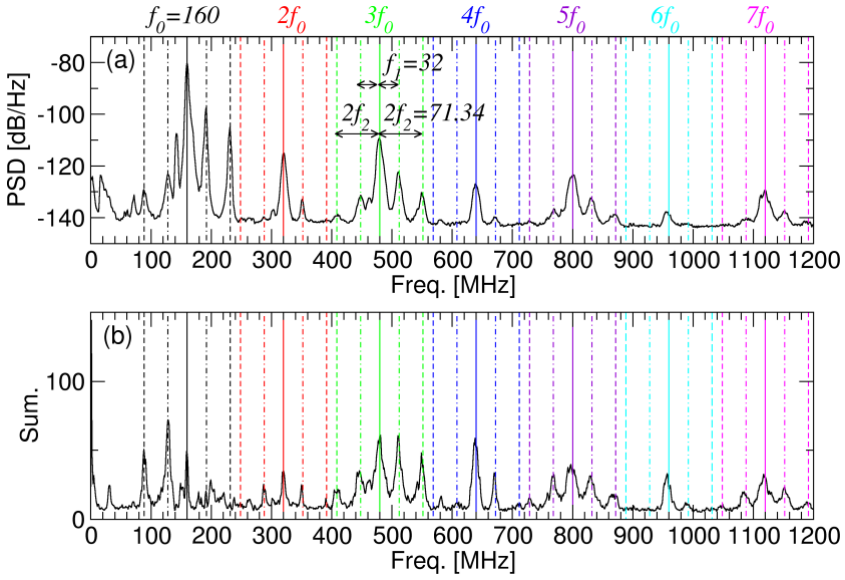

Figure 11: (a) Power spectrum density averaged around t=3.3545, detected at the 10-O port viewing a horizontally long cross section. (b) Sum of the auto bicoherence. Intense peaks appear around f_0=160 MHz and their harmonics indicated by solid lines with sidebands whose gap frequencies, f_1 =32 MHz indicated by dot-dashed lines and $2f_2$ =71.34 MHz indicated by dashed lines.

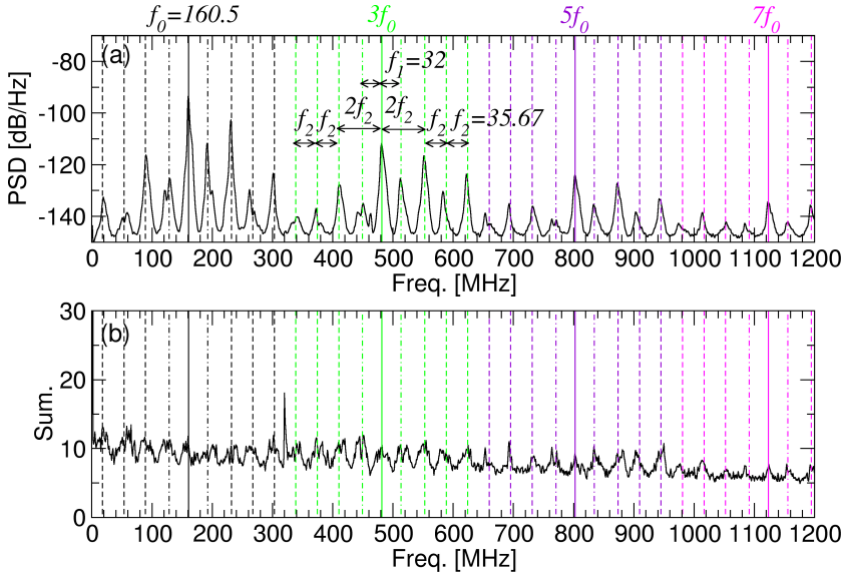

*Figure 12: (a) Power spectrum density averaged around t=3.3545, detected at the 9.5-L port viewing a longitudinal cross section. (b) Sum of the auto bicoherence. Intense peaks appear around f_0=160.5 MHz and their harmonics indicated by solid lines with sidebands whose gap frequencies, f_1 =32 MHz indicated by dot-dashed lines, and mf_2=m*35.67 MHz indicated by dashed lines, where m=2,3,4.*

During the largest burst, complex frequency spectrums are detected by both antennas. It looks that the gaps of sidebands are not constant. Panels (a)/(b) of Fig. 10 show the auto-bicoherence of electric fluctuations detected at

the 10-O/9.5-L ports viewing near the horizontal long/longitudinal cross section. In panel (a), strong interactions are seen with intervals approximately 160 MHz with sideband gaps. In panel (b), strong interactions are shown along F1, F2 ~ 320 MHz, and F2 ~ 70 MHz. Figs. 11 and 12 show frequency spectrograms of the power and bicoherence of electric fluctuations detected at each port. There are two gap frequencies of sidebands around f_0 and its harmonics, i.e. f_1 = 32 MHz and mf_2 = 35.67 MHz. Notably, it was found that f_0 shown in the spectrums is slightly different as f_0=160 MHz detected at the 10-O port viewing a horizontally long cross section, and f_0=160.5 MHz detected at the 9.5-L port viewing a longitudinal cross section.

3. DISCUSSION

3.1. Locations of corresponding wave resonances during the largest burst

In the previous PIC simulation study [14], it was derived that the ion cyclotron wave (ICW) at a constant frequency $l\Omega_{ci}$ is excited when the lower hybrid frequency approaches $l\Omega_{ci}$, and the $(l\text{-}1)\,\Omega_{ci}$ ICW excited by energetic ions couples with the bulk ion Bernstein mode whose dispersion curve connects to ω_{LH} for l=5, 6, 7. These characteristic are similar to experimental observation of stair-like frequency shift of intense peak frequency with increase of the background density. We examined the locations of the lower hybrid resonance (LHR) corresponding to f_0 = 160 MHz, and 160.5 MHz and ion cyclotron resonances (ICRs) corresponding to f_1=32 MHz, and f_2=35.5 MHz with assuming a hollow density profile where the electron density is $0.0436\times10^{19}\mathrm{m}^{-3}$ at the magnetic axis. We found that the LHR corresponding to f_0 = 160 MHz overlaps with an ICR of f_1=32 MHz at the poloidal cross-section 8 and 26 degrees away from the horizontally long cross section namely dual resonance 1 (DR1) as shown in panel (a) ns(b) of Fig. 13. And the LHR corresponding to f_0 = 160.6 MHz also overlaps with another ICR of f_2=35.67 MHz at the horizontally long and longitudinal cross sections, namely DR2 as shown in panels (c) and (d) of Fig. 13. Note that there are relationships such as $5f_1$= 160 MHz ~160.5 MHz, $9f_2$= 321 MHz= 2×160.5 MHz. Based on simulation results, the excitation of intense lower hybrid and cyclotron harmonic emissions can be expected in DR1 where the lower hybrid frequency is around 160 MHz that is almost corresponds the 5th harmonic of the ion cyclotron frequency of 32 MHz. We found that DR2 exist near $\rho = 0.2$ at the horizontally ling cross section and $\rho = 0.6$ at the longitudinal cross section, where ρ is the normalized minor radius. DR1 exists at poloidal cross sections 8° distant from the horizontally long and longitudinal cross sections. The toroidal and poloidal helical polarities of LHD are L=2 and M=10. The double resonance conditions of DR1 and DR2 appear periodically every 18° in the torus.

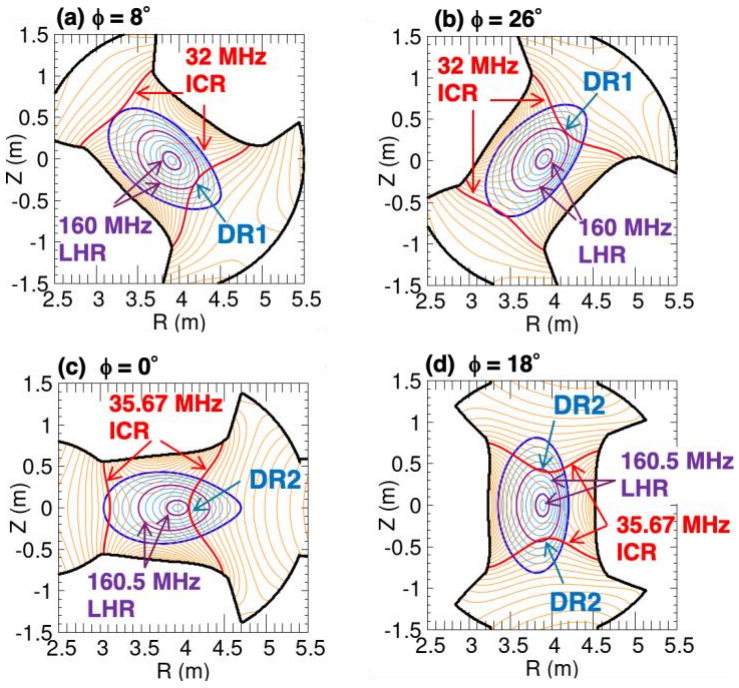

Figure 13: (a), (b)Locations of the LHR of f_0 = 160 MHz overlapping with the ICR of f_1=32 MHz, namely DR1 8° and 26° distant from the horizontally long cross section; (c), (d) Locations of the LHR of f_0 = 160.5 MHz overlapping with the ion cyclotron resonance of f_2=35.67 MHz, namely DR2. The blue lines represent magnetic flux surfaces, while the orange lines represent magnetic field strength contours.

3.2. Discussion about the mechanism of large bursty enhancement

At this stage, this remains a hypothesis, but we consider that waves traveling between these DRs interfere with each other as summarized in Fig.14, leading to nonlinear increase in wave amplitude. Like the vibrato tone in music scene, application of slightly different frequency oscillations can cause nonlinear enhancement of the fluctuation intensity. Actually, we found that at the different locations, f_0 are slightly different during the largest burst by the power spectrum and bicoherence analyses. To verify this hypothesis, both wave propagation analysis and analysis with introducing a mathematical model described with some nonlinear equations such as the Mathieu equation or Hill equation are required.

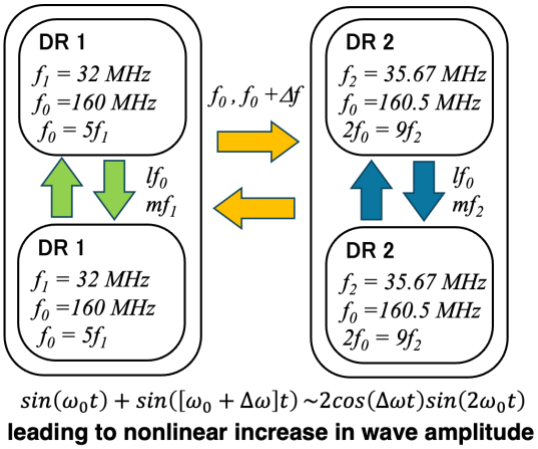

Figure 14: Conceptual diagram of waves propagating between the dual resonances which cause bursty amplitude modulation at twice the resonant frequencies

4. SUMMARY

This study demonstrated the potential to enhance the growth of waves at the LH frequency and its harmonic wave ranges, as well as waves at the IC frequency and its harmonic frequencies, by establishing multiple dual resonances at distinct locations in the presence of energetic ions. It has been suggested that excitations of lower hybrid range waves which have slightly different frequencies can lead large bursty enhancement of the wave amplitude. Large enhancement of IBWs, and ICWs have potential to perform efficient resonant heating of bulk ions. This opens the possibility of exploring scenarios for bulk ion heating in fusion MCF plasmas through resonant heating induced by these spontaneously excited waves.

ACKNOWLEDGEMENTS

The authors would like to thank the technical staff of the LHD group at the National Institute for Fusion Science for their helpful support during this work. The data supporting the findings of this study are available in the LHD experiment data repository at https://doi.org/10.57451/lhd.analyzed-data. This work was supported by JSPS KAKENHI Grant Number 23K03363.

REFERENCES

[1] FISCH N. J. and RAX J.-M., Physical Review Letters, **69**, (1992) 612-615
[2] OCHS I. E., BERTELLI N., and FISCH N. J, Physics of Plasmas, **22**, (2015) 112103
[3] FISCH N. J. and HERRMANN M. C., Nuclear Fusion **35** (1995) 1753
[4] ROMANELLI F., and CARDINALI A., Nuclear Fusion **60** (2020) 036025
[5] COOK, J. W. S., DENDY, R. O., CHAPMAN, S. C., Physical Review Letters, **118**, (2017) 185001
[6] SAITO K., KASAHARA H., SEKI T., et al., Fusion Engineering and Design **84** 1676-1679, (2009)
[7] SAITO K., KUMAZAWA R., SEKI R., Plasma Science and Technology **5**, (2013), 209-212,
[8] SAITO K., IGAMI H., TOIDA M., et al., Plasma and Fusion Research **13,** (2018), 3402043
[9] REMAN B. C. G., DENDY R. O., AKIYAMA T., et al., Nuclear Fusion **59**, (2019), 096013
[10] REMAN B. C. G., DENDY R. O., AKIYAMA T., et al., Nuclear Fusion **61**, (2021), 066023
[11] REMAN B. C. G., DENDY R. O., IGAMI H., et al., Plasma Physics and Controlled Fusion **64**, (2022) 085005
[12] IGAMI H., SAITO K., REMAN B. C. G. et al., submitted to Journal of Fusion Energy
[13] TOIDA M., SAITO K., IGAMI H., et al., Plasma and Fusion Research **13**, (2018), 343015
[14] TOIDA M., IGAMI H., SAITO K., et al., Plasma and Fusion Research **14**, (2019), 340112
[15] KOTANI T., TOIDA M., MORITAKA T., and TAGUCHI S., Physical Review E **108**, (2023), 035208